

# Encapsulated Magnetic Nanoparticles as Supports for Proteins and Recyclable Biocatalysts

Aimee R. Herdt, Byeong-Su Kim, and T. Andrew Taton\*

University of Minnesota, Department of Chemistry, 207 Pleasant Street SE, Minneapolis, Minnesota 55455.

Received July 14, 2006; Revised Manuscript Received November 13, 2006

This paper describes the bioconjugation of histidine-tagged enzymes and other proteins to the surface of composite “magnetomicelles” consisting of magnetic  $\gamma$ -Fe<sub>2</sub>O<sub>3</sub> nanoparticles encapsulated within cross-linked polystyrene-*block*-polyacrylate copolymer micelle shells. Free carboxylic acid groups on the magnetomicelle surface were converted to Cu<sup>2+</sup>-iminodiacetic acid (IDA) for protein capture. The conjugation of T4 DNA ligase and enhanced green fluorescent protein to magnetomicelles revealed that proteins were captured with a high surface density and could be magnetically separated from reaction mixtures and subsequently released from the nanoparticle surface. Additionally, bioconjugation of T7 RNA polymerase yielded a functional enzyme that maintained its biological activity and could be recycled for up to three subsequent transcription reactions. We propose that protein–magnetomicelle bioconjugates are effective for protein bioseparation and enzymatic recycling and further strengthen the idea that nanoparticle surfaces have utility in protein immobilization.

## INTRODUCTION

Protein-modified particles (1), both microparticles and nanoparticles, have many biotechnological uses, including protein separation and purification, protein detection and analysis, in vivo imaging, bioelectrodes and biosensors, and biocatalytic transformations (2–7). Particle-bound enzymes are of special interest as recyclable catalysts. In principle, magnetic nanoparticles should be excellent solid supports for enzymes (8); nanoparticle supports inherently maximize the surface area available for enzyme attachment, and magnetic nanoparticles with sufficient magnetization are easily recovered from aqueous suspension by applying a static magnetic field. One significant challenge to practical use of magnetic nanoparticles as enzyme supports is the availability of general bioconjugate chemistries for connecting proteins to particles. Current methods for attaching proteins to particles include physical adsorption/deposition (9, 10), entrapment (11, 12), cross-linking (5), and covalent attachment (13). One attractive strategy for specifically conjugating proteins to particles uses fusion tags to attach a specific locus, usually the N- or C-terminus, to reactive or coordinating groups on the particle surface (14–17). For example, Xu and co-workers recently demonstrated that hexahistidine (His<sub>6</sub>)-tagged GFP could be selectively captured onto nitriloacetic acid (NTA)-modified FePt (18) or M/Fe<sub>2</sub>O<sub>3</sub> (M = Co or SmCo<sub>5,2</sub>) (19) nanoparticles when appropriate ligands were covalently installed on the particle surfaces.

In order to control the stability and surface functionality of magnetic nanoparticles, our group has developed a method for the encapsulation of hydrophobic  $\gamma$ -Fe<sub>2</sub>O<sub>3</sub> particles ( $d = 10.9$  nm) in amphiphilic polystyrene<sub>250</sub>-*block*-poly(acrylic acid)<sub>13</sub> (PS<sub>250</sub>-*b*-PAA<sub>13</sub>) block copolymer (20). The outer PAA block of the micelles renders these nanostructures water-soluble and displays carboxylic acid groups used to (1) permanently fix the micelle shell with EDC-activated 2,2'-(ethylenedioxy)bis(ethylamine) cross-linker and (2) facilitate the attachment of biomolecules. Herein, we demonstrate the covalent immobilization of proteins onto these hybrid nanoscale materials, termed

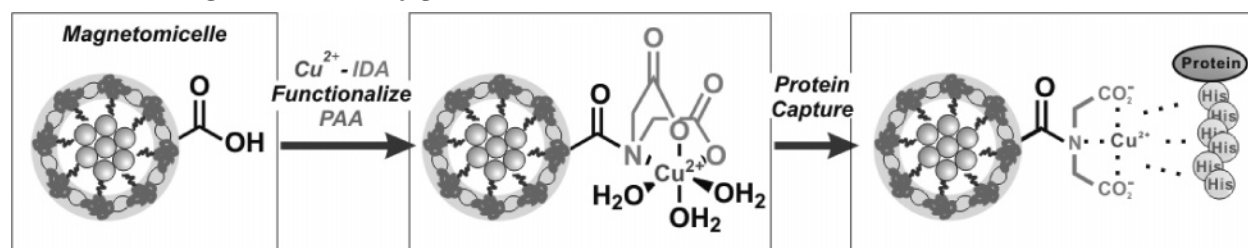
“magnetomicelles”, by attaching iminodiacetic acid (IDA) to the micelle surface, and use the functionalized Cu<sup>2+</sup>-IDA magnetomicelles to selectively capture His<sub>6</sub>-tagged proteins (Scheme 1) (18, 21). We establish that the encapsulated magnetic nanoparticles are suitable for biological environments and permit the external manipulation of conjugated biomolecules. Specifically, we report the bioseparation of His<sub>6</sub>-tagged T4 DNA ligase (T4 DNAL) and enhanced green fluorescent protein (EGFP). In addition, we show that T7 RNA polymerase (T7 RNAP) maintains enzyme activity while conjugated to magnetomicelles and that the enzyme bioconjugate is recoverable for recycled enzyme use.

## EXPERIMENTAL PROCEDURES

**Magnetomicelle Preparation and Functionalization.** Magnetomicelles were prepared as previously reported (20). Briefly, magnetomicelles were prepared from 10.9 nm  $\gamma$ -Fe<sub>2</sub>O<sub>3</sub> magnetic nanoparticles ( $[\gamma\text{-Fe}_2\text{O}_3]_{\text{initial}} = 0.30$  mg/mL in 50:50 DMF/THF) and PS<sub>250</sub>-*b*-PAA<sub>13</sub> ( $[\text{PS}_{250}\text{-}b\text{-PAA}_{13}]_{\text{final}} = 2.0 \times 10^{-2}$  mg/mL). Assembled, copolymer-coated particles were exposed to 1-ethyl-3-(3-dimethylaminopropyl)-carbodiimide (EDC) to activate 50% of the PAA block carboxylates, followed by 2,2'-(ethylenedioxy)bis(ethylamine) to cross-link these carboxylates. For IDA functionalization, 5.0 mL of magnetomicelle solution (effective carboxylic acid groups in PAA block =  $2.41 \times 10^{-8}$  mol) was mixed with 21.5  $\mu$ L of freshly prepared EDC solution (1.0 mg/mL in H<sub>2</sub>O, 3.0 equiv to carboxylic acid groups in the PAA block) with vigorous stirring. After 30 min of activation, 31.4  $\mu$ L of *N*-hydroxysulfosuccinimide sodium salt (sulfo-NHS) (1.0 mg/mL in H<sub>2</sub>O, 6.0 equiv to carboxylic acid groups in the PAA block) was added to the suspension. Solutions were stirred for 1.5 h, and the suspension was added dropwise to 32  $\mu$ L of iminodiacetic acid (IDA) (1.0 mg/mL in H<sub>2</sub>O, 10 equiv to carboxylic acid groups in the PAA block) in 1.0 mL of 10 mM Na<sub>2</sub>CO<sub>3</sub>/NaHCO<sub>3</sub> buffer (pH 9.5) (22). The solution was vigorously mixed for 24 h at room temperature and dialyzed against diH<sub>2</sub>O (Spectra/Por 4 Regenerated Cellulose Membrane, MWCO = 12–14K) over 48 h. To this solution was added 7.2  $\mu$ L of aqueous CuSO<sub>4</sub>·5H<sub>2</sub>O (10 mg/mL in H<sub>2</sub>O, 10 equiv of carboxylic acid groups in the PAA block), and the mixture was

\* Author to whom correspondence should be addressed. E-mail: taton@chem.umn.edu.

Scheme 1. Protein–Magnetomicelle Bioconjugation



allowed to stand for 3 h to load IDA groups with  $\text{Cu}^{2+}$ ; excess reagents were removed with extensive dialysis.

#### Characterization of Functionalized Magnetomicelles.

Transmission electron microscopy (TEM) images were obtained on a JEOL 1210 electron microscope equipped with a Gatan video camera and a Gatan Multiscan CCD camera ( $1024 \times 1024$  pixels). Magnetomicelle solutions were dropped onto 300-mesh Formvar-graphite-coated copper TEM grids (Electron Microscopy Science, Hartfield, PA) and air-dried for TEM imaging. All images were obtained at an operating voltage of 120 kV.

**Protein Preparation, Purification.** Recombinant T4 DNA ligase (BL21(DE3)p-lysS, p3H11) (23), EGFP (pBAD-18-Cm) (24), and T7 RNA polymerase (M15:pDMI.1, p6HRNAP) (25), all containing His<sub>6</sub> fusion tags, were overexpressed in *E. coli* according to previously published protocols. Proteins were purified by affinity chromatography using Ni<sup>2+</sup>-NTA-agarose resin (Qiagen) and eluted with imidazole-containing buffer. Product protein solutions were buffer-exchanged and concentrated by centrifugal dialysis using Centriprep YM-10 tubes (Amicon, Bedford, MA) and stored at  $-20^\circ\text{C}$ . Proteins were analyzed by 8% SDS-PAGE and their concentrations estimated by standard BCA protein assay.

**Bioconjugate Preparation and Magnetic Separation.** Suspensions of  $\text{Cu}^{2+}$ -IDA magnetomicelles were mixed with His<sub>6</sub>-tagged proteins in Eppendorf tubes for 2 h at  $4^\circ\text{C}$ . Magnets (NdFeB magnet, 0.14 T) were applied to the bottom and one side edge of the tubes for 1 h, and the supernatant (top 70% of solution) was pipetted away, in order to isolate the magnetomicelle–protein conjugates from unconjugated, free protein. The magnetomicelle–protein bioconjugates were then washed two to four times with diH<sub>2</sub>O prior to protein analysis, elution, or enzymatic reaction. To wash, the magnet was removed from the bottom of the Eppendorf tube, residue was resuspended in an equal volume diH<sub>2</sub>O, the magnets were reapplied for 1 h, and the supernatant (top 50%) was pipetted away.

**T4 DNA Ligase–Magnetomicelle Assay.** 450  $\mu\text{L}$  of  $\text{Cu}^{2+}$ -IDA magnetomicelle solution was mixed with T4 DNAL and 10% SDS for a total reaction volume of 500  $\mu\text{L}$ . Reactions were treated as described above in Bioconjugate Preparation and Magnetic Separation. T4 DNAL could be eluted from the magnetomicelles by resuspending magnetically separated residue in 75  $\mu\text{L}$  1 M imidazole, followed by a round of magnetic separation. The flow-through, washes, and final elution fraction were dialyzed overnight against diH<sub>2</sub>O using Slide-A-Lyzer Mini Dialysis units (Pierce, Rockford, IL) at  $4^\circ\text{C}$ . Dialyzed samples were lyophilized to dryness and resuspended in 10  $\mu\text{L}$  for gel analysis by 8% SDS-PAGE. In control experiments, magnetomicelles were treated as described above, except that IDA and  $\text{Cu}^{2+}$  were omitted.

**GFP–Magnetomicelle Assay.** 200  $\mu\text{L}$  of  $\text{Cu}^{2+}$ -IDA magnetomicelle solution was mixed with EGFP. Reactions were treated as described in Bioconjugate Preparation and Magnetic Separation. All washes and the final 60  $\mu\text{L}$  fraction of EGFP–magnetomicelle bioconjugates were resuspended to 140  $\mu\text{L}$  for fluorescence analysis. EGFP–magnetomicelle data reported is the average of six individual experiments. The steady-state

fluorescence measurements were obtained with a Quantamaster Fluorimeter (PTI London, Ontario) at room temperature, using an excitation wavelength of 395 nm and emission and excitation slit widths of 2 nm. In all experiments, the raw average of two emission scans was reported. An EGFP fluorescence calibration curve was generated by magnetically separating 200  $\mu\text{L}$  of nonfunctionalized magnetomicelle suspension, then removing 60  $\mu\text{L}$  of the supernatant. The resulting 140  $\mu\text{L}$  of micelle solution was mixed with known amounts of EGFP and the fluorescence intensity measured.

**T7 RNA Polymerase Activity.** 200  $\mu\text{L}$  of  $\text{Cu}^{2+}$ -IDA magnetomicelle solution was mixed with T7 RNAP. Reactions were treated as described in Bioconjugate Preparation and Magnetic Separation. The final 60  $\mu\text{L}$  fraction of T7 RNAP–magnetomicelle bioconjugates were added to transcription reactions, performed at  $37^\circ\text{C}$  for 4 h, in the presence of  $10\times$  transcription buffer (0.4 M Tris·Cl, pH 8.0, 60 mM MgCl<sub>2</sub>, 0.01 M spermidine, 0.1% 1090 Triton, BSA and DTT), 4 mM each NTPs, 1  $\mu\text{M}$  template DNA, 20 mM MgCl<sub>2</sub>, and 10 mM DTT for a final reaction volume of 100  $\mu\text{L}$ . Template DNA was (i) a 155-mer, PCR-generated synthetic template containing the DNA sequence for the T7 RNAP promoter or (ii) plasmid DNA (3.4 kb), which contains the T7 RNA promoter and the DNA template for *E. coli* tRNA<sup>Pro</sup> RNA (76-mer) (26). Plasmid DNA was digested with *Bst*NI and gel-purified prior to transcription. For T7 RNAP–magnetomicelle recycling experiments, after the first transcription reaction, the reaction solution was magnetically separated and 70% of the free reaction solution was removed (70  $\mu\text{L}$ ) for gel analysis. The remaining 30  $\mu\text{L}$  of T7 RNAP–magnetomicelle bioconjugates were resuspended to 120  $\mu\text{L}$  with diH<sub>2</sub>O and treated according to Bioconjugation Preparation and Magnetic Separation, described above. The final 60  $\mu\text{L}$  was reused in a second transcription reaction. Transcription products (RNA) were analyzed by denaturing 12% PAGE. Control experiments were performed as described above, except that all the fractions were collected without the application of the magnets. In addition, reactions were run with unconjugated T7 RNAP and T7 RNAP mixed with magnetomicelles that were not washed from T7 RNAP free in solution.

## RESULTS

On the basis of our previous studies on the synthesis and functionalization of copolymer micelle-encapsulated nanoparticles (20, 27, 28), we anticipated that  $\gamma\text{-Fe}_2\text{O}_3$  magnetomicelles would be excellent supports for proteins. Encapsulation of  $\gamma\text{-Fe}_2\text{O}_3$  magnetic nanoparticles within cross-linked surfactant shells makes it possible to take advantage of the nanoparticles' intrinsic properties without the need to develop specific chemistries for directly attaching proteins to the nanoparticle surface. The surfactant shell also stabilizes the particles to physical and chemical manipulation in biological buffers and protects proteins from direct contact with the core nanoparticle surfaces. In this study, we used magnetomicelles in which 50% of the PAA carboxylates were cross-linked, leaving the other 50% available for bioconjugation.

The bioconjugate chemistry used in this study is based on immobilized metal affinity chromatography (IMAC), a common

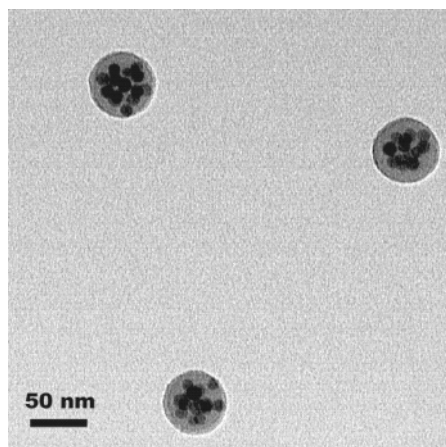


**Figure 1.** Representative TEM micrograph of  $\text{Cu}^{2+}$ -IDA functionalized magnetomicelles. Multiple  $\gamma\text{-Fe}_2\text{O}_3$  nanoparticles are confined within each polymer micelle core, and the average  $\text{Cu}^{2+}$ -IDA magnetomicelle diameter is 50 nm.

technique for the purification of recombinant proteins (29, 30). In IMAC,  $\text{His}_6$ -protein fusions are initially bound to  $\text{Ni}^{2+}$ - or  $\text{Co}^{2+}$ -loaded nitriloacetic acid (NTA) groups on functionalized resin and can be subsequently eluted from the support by exposure to imidazole solution. Interactions between  $\text{His}_6$  tags and metal-NTA groups have recently been used to capture proteins on the surfaces of various types of nanostructures, including gold (21) and magnetic nanoparticles (18, 19) and magnetic nanorods (31). We chose to functionalize magnetomicelles with  $\text{Cu}^{2+}$ -IDA rather than  $\text{Ni}^{2+}$ - or  $\text{Co}^{2+}$ -NTA due to its higher binding affinity for the polyhistidine fusion tag (32, 33). Magnetomicelle carboxylates were converted to IDA groups via EDC coupling. Particles were then exposed to  $\text{Cu}^{2+}$  and washed to prepare them for protein loading. TEM micrographs of  $\text{Cu}^{2+}$ -IDA functionalized magnetomicelles appeared identical to those taken prior to functionalization (Figure 1). Further characterization by X-ray photoelectron spectroscopy (XPS) confirmed the presence of copper in dialyzed  $\text{Cu}^{2+}$ -IDA magnetomicelle preparations. By contrast, control samples in which EDC was omitted from the magnetomicelle functionalization exhibited no XPS peak corresponding to copper (data not shown). This experiment indicates that IDA functionalization was required to bind  $\text{Cu}^{2+}$ . Suspensions of  $\text{Cu}^{2+}$ -IDA magnetomicelles were stable for at least several months but were typically bound to proteins soon after synthesis. Assuming that functionalization with IDA was similar to that of primary amines studied previously in our group, we estimate that several hundred  $\text{Cu}^{2+}$ -IDA molecules can be attached to the surface of a single, 50-nm magnetomicelle (20).

We initially evaluated  $\text{Cu}^{2+}$ -IDA magnetomicelles as protein supports by using them to capture  $\text{His}_6$ -tagged T4 DNA ligase (T4 DNAL). These experiments were designed to mimic standard, column-based IMAC protein purification protocols. Proteins were first captured by suspended nanoparticles, which were washed to remove unbound protein. Then, an IMAC-competing ligand, imidazole, was added to elute the protein from its nanoparticle supports (34). In all experiments, excess T4 DNAL was added to the functionalized magnetomicelles to saturate the particles with protein. Numerous cycles of magnetic separation and washing were used to remove unbound protein. The supernatant recovered from each step of protein bioconjugation and purification was analyzed by gel electrophoresis (Figure 2a). Excess unbound protein was recovered only in initial washing steps; subsequent magnetic separations and redispersion showed no loss of bound T4 DNAL to the supernatant. Elution with imidazole, however, yielded a single band on the SDS-PAGE gel corresponding to pure T4 DNAL.

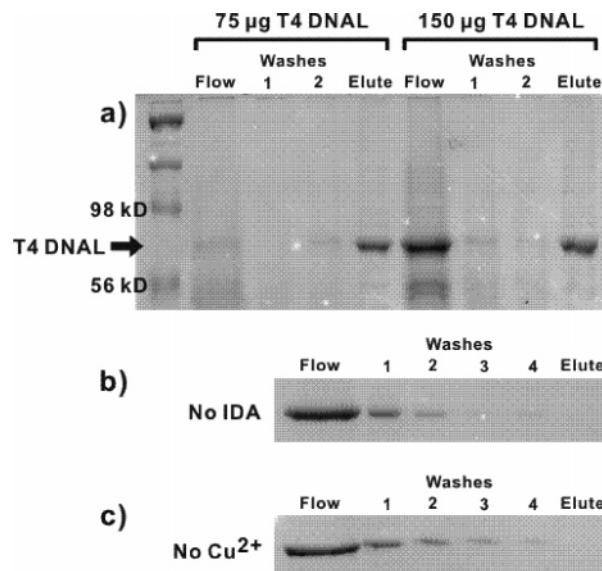


**Figure 2.** SDS-PAGE gel of T4 DNA ligase (68 kD) captured and isolated from  $\sim 2 \times 10^{11}$  magnetomicelles (400  $\mu\text{L}$  magnetomicelle solution), where (a) micelles were conjugated with varying amounts of T4 DNA ligase, or where (b) IDA or (c)  $\text{Cu}^{2+}$  was omitted from the preparation. Flow: Unbound material collected from supernatant after initial conjugation. Washes: Material collected from  $\text{dH}_2\text{O}$  wash steps. Elute: Material collected after exposure to 500  $\mu\text{M}$  imidazole.

The binding capacity for T4 DNAL was dependent on the magnetomicelle concentration, such that the amount of T4 DNAL captured by equal suspensions of magnetomicelles was qualitatively reproducible, regardless of the amount of protein initially mixed with the nanoparticles. For example, magnetomicelle preparations mixed with 75 or 150  $\mu\text{g}$  of T4 DNAL eluted similar quantities of protein after T4 DNAL-magnetomicelle purification (Figure 2a, elute lanes; additional data not shown).

Control experiments verified the specificity of the interaction between the  $\text{Cu}^{2+}$ -loaded IDA groups and the  $\text{His}_6$  tags. In general, proteins lacking  $\text{His}_6$  fusion tags did not bind to the surfaces of magnetomicelles. As a result, when particles were mixed with impure preparations of T4 DNAL, the imidazole-eluted protein was always observed to be more pure than the starting material by SDS-PAGE analysis (Figure 2a; additional data not shown). In addition, control experiments in which magnetomicelles were either not functionalized with IDA or not loaded with  $\text{Cu}^{2+}$ , exposed to T4 DNAL, and then subjected to elution conditions showed negligible protein capture. Instead, the T4 DNAL mixed with these preparations was recovered from the reaction solution during magnetic separation and washing (Figure 2b,c). This data confirms that the interaction between the particle-bound  $\text{Cu}^{2+}$ -IDA groups and the  $\text{His}_6$  tag is highly specific. Similar work on monolithic, PAA-coated surfaces that had been modified with metal-NTA groups has shown low nonspecific binding in the absence of metal or ligand (35).

In order to quantify the protein bound to magnetomicelles, we analyzed particles conjugated to  $\text{His}_6$ -tagged enhanced green fluorescent protein (EGFP). The intrinsic fluorescence of GFP has been previously used in protein attachment to surfaces (36, 37), supported membranes (38), and particles (18, 39). Here, to further quantify the effectiveness of magnetomicelle protein loading, as well as to verify protein integrity after conjugation,  $\text{His}_6$ -tagged EGFP was captured by the magnetomicelles. As with  $\text{His}_6$ -T4 DNAL, gel electrophoresis experiments demonstrated that  $\text{His}_6$ -EGFP could be bound to the magnetomicelle surface and eluted with imidazole (34).

The conjugation and surface density of  $\text{His}_6$ -EGFP was also monitored by fluorescence spectroscopy. Overall, the fluores-

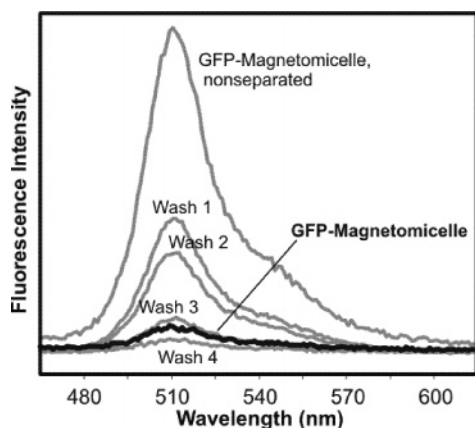


**Figure 3.** Fluorescence spectra of GFP–magnetomicelles, prior to magnetic separation, after all subsequent washes and after recovery of the bioconjugate solution. Bioconjugates were washed until the supernatant exhibited no significant fluorescence (Figure 3). Then, the fluorescence signal from the EGFP–magnetomicelle bioconjugates was measured. When limiting amounts of His<sub>6</sub>-EGFP were added to the preparation, the fluorescence intensity of these suspensions increased with increasing EGFP concentration. At the saturating concentration of His<sub>6</sub>-EGFP, we estimate that 300 molecules of EGFP are attached to each 50-nm-diameter magnetomicelle in solution, based on the final fluorescence intensity of the suspension, or one molecule of EGFP per 26 nm<sup>2</sup> of particle surface. Given that GFP has a footprint of 12 nm<sup>2</sup> (40), this corresponds to a fairly high surface density of attached protein. The high density of conjugated EGFP molecules is consistent with our previous study, which indicated that around 600 molecules of NH<sub>2</sub>-(ethylene glycol)<sub>5</sub>-fluorescein functionalized the surface of a single magnetomicelle (20). The fluorescence intensity of the conjugates also suggests that EGFP remains intact while conjugated to the surface of the magnetomicelles, due to the retention of the protein's intrinsic fluorescence. Attaching GFP to magnetomicelles gives us a quantitative way to measure the magnetomicelle–protein loading capacity.

cence spectrum of EGFP was not affected by conjugation to the particles. After mixing His<sub>6</sub>-EGFP with the magnetomicelle suspension, the mixture was magnetically separated and washed until the supernatant exhibited no significant fluorescence (Figure 3). Then, the fluorescence signal from the EGFP–magnetomicelle bioconjugates was measured. When limiting amounts of His<sub>6</sub>-EGFP were added to the preparation, the fluorescence intensity of these suspensions increased with increasing EGFP concentration. At the saturating concentration of His<sub>6</sub>-EGFP, we estimate that 300 molecules of EGFP are attached to each 50-nm-diameter magnetomicelle in solution, based on the final fluorescence intensity of the suspension, or one molecule of EGFP per 26 nm<sup>2</sup> of particle surface. Given that GFP has a footprint of 12 nm<sup>2</sup> (40), this corresponds to a fairly high surface density of attached protein. The high density of conjugated EGFP molecules is consistent with our previous study, which indicated that around 600 molecules of NH<sub>2</sub>-(ethylene glycol)<sub>5</sub>-fluorescein functionalized the surface of a single magnetomicelle (20). The fluorescence intensity of the conjugates also suggests that EGFP remains intact while conjugated to the surface of the magnetomicelles, due to the retention of the protein's intrinsic fluorescence. Attaching GFP to magnetomicelles gives us a quantitative way to measure the magnetomicelle–protein loading capacity.

In order for magnetic nanoparticles to be useful as supports for enzymes, the bound enzyme must maintain its native activity even after repeated physical manipulation. A variety of enzymes have been used as models for evaluating the activity of particle-bound enzymes, including *Candida rugosa* lipase (41), horseradish peroxidase (21, 42), proteases (43, 44), and glucose oxidase (3). To test the use of magnetomicelles as recyclable supports for enzymes used in molecular biology, we used magnetomicelles in conjunction with an enzyme routinely used for the *in vitro* transcription of RNA, T7 RNA polymerase (T7 RNAP). Like most enzymes in molecular biology protocols, T7 RNAP is by far the most expensive reagent used in a transcription reaction, and we expected that attaching the enzyme to magnetomicelles would allow it to be recycled after use. However, T7 RNAP is susceptible to inhibition by a variety of reaction contaminants (45), and so we first tested whether transcription was inhibited by the magnetomicelle supports. Cu<sup>2+</sup>-IDA magnetomicelles (with no protein attached) were added to otherwise ordinary transcription reactions of two separate dsDNA templates: a 155-nt, linear template that generates a 135-mer mRNA, and 3.4 kb plasmid that yields the 76-mer tRNA<sup>P<sup>ro</sup></sup> (26). Gel electropherograms of the RNA

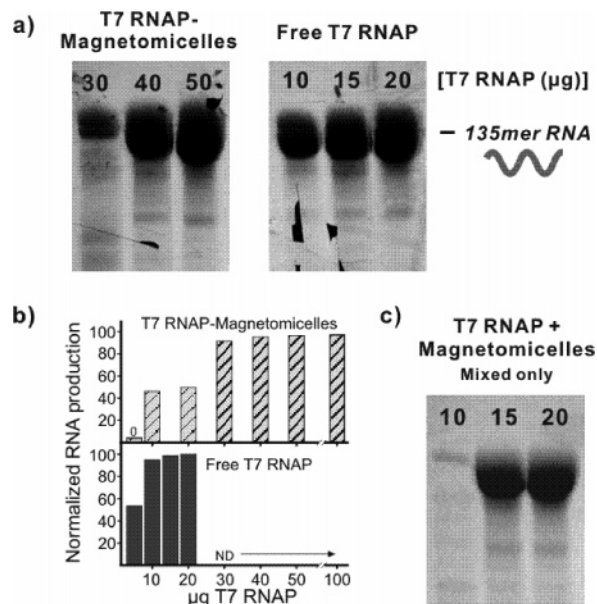


**Figure 4.** (a) Representative urea-PAGE gel images of RNA produced by T7 RNAP–magnetomicelles or free T7 RNAP, at concentrations where the enzyme was the limiting reagent. (b) Graphical analysis of densitometry studies of numerous gel images. Transcription data for free T7 RNAP at concentrations above 20 µg were not determined (ND), because the maximum level of RNA production was reached by 20 µg of enzyme. The data was normalized, such that the RNA generated with 20 µg of free T7 RNAP was set to 100%. No RNA was detected with 5 µg of T7 RNAP bound to the magnetomicelles. (c) Urea-PAGE gel of RNA produced when magnetomicelle suspension was added to a transcription reaction already in progress.

products produced in the absence or presence of Cu<sup>2+</sup>-IDA magnetomicelles were indistinguishable (data not shown).

Additional experiments with magnetomicelle-bound RNA polymerase demonstrate that these materials are active, recoverable catalysts for transcription. Magnetomicelles were loaded with His<sub>6</sub>-T7 RNAP, washed exhaustively, and used in place of free T7 RNAP to transcribe the two DNA templates described above. Conjugated T7 RNAP successfully transcribed both linear and plasmid DNA to RNA under standard reaction conditions (34). Cu<sup>2+</sup>-IDA magnetomicelles that had been incubated with T7 RNAP that lacked a His<sub>6</sub> tag, by contrast, failed to catalyze DNA transcription (34). We conclude that, as was true for His<sub>6</sub>-T4 DNAL and His<sub>6</sub>-GFP, the hexahistidine tag is required to conjugate T7 RNAP to Cu<sup>2+</sup>-IDA magnetomicelles and non-specific adsorption of active catalyst was not significant.

In order to relate the activity of T7 RNAP–magnetomicelles to that of free T7 RNAP, we compared the amount of RNA product generated in side-by-side reactions using both catalysts. Experiments were conducted in which the enzyme was a limiting reagent for RNA production, and in all cases, the amount of DNA template was held constant at 1 µM. As is true for T7 RNAP alone, increasing concentrations of RNAP-loaded magnetomicelles increased transcription efficiency (Figure 4a). Collectively, using densitometry to quantify the amount of RNA produced, these transcription assays reveal that efficient transcription requires 3–4 times the amount of T7 RNAP to be conjugated to the magnetomicelle surfaces versus free enzyme in solution (Figure 4b). However, we found that any manipulation of the standard transcription reaction, including adding magnetomicelles to a transcription reaction already in progress, causes a slight decrease in RNA production (Figure 4c). As a result, it is possible that the magnetomicelle solution is slightly inhibitory to T7 RNAP, regardless of its bound or unbound state, or causes RNA degradation, perhaps due to the presence of RNases.

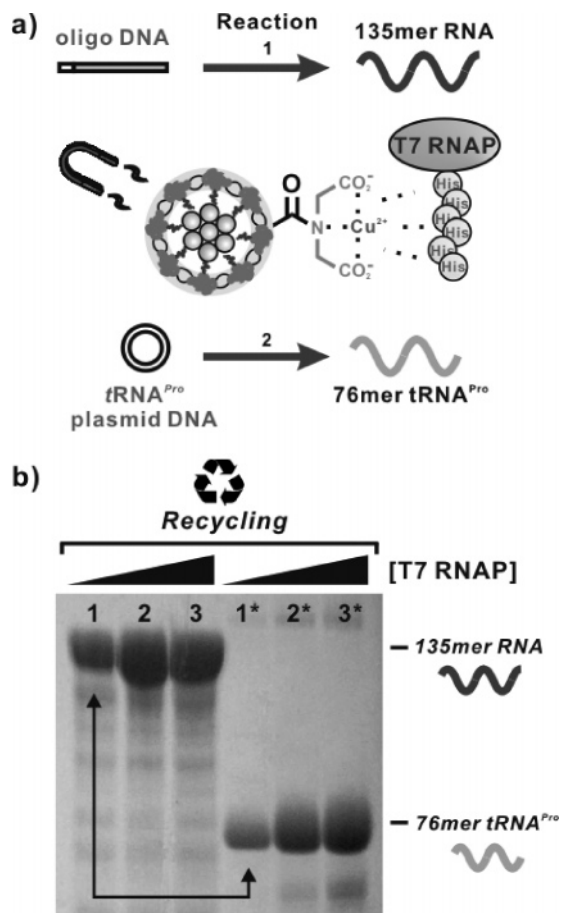


**Figure 5.** (a) T7 RNAP–magnetomicelle recycling scheme. (b) Urea-PAGE gel of RNA produced by T7 RNAP–magnetomicelles. Starred lanes represent the second reaction performed with the recycled T7 RNAP–magnetomicelle bioconjugates from the similarly numbered but unstarred lanes. The concentration of T7 RNAP conjugated to the magnetomicelles increased from lanes 1–3.

Consequently, to further justify the utility of our protein–magnetomicelle bioconjugates, we tested the recyclability of the conjugates. Recycling biologically relevant enzymes, for as little as one or two subsequent assays, could greatly reduce experimental times and costs. To test whether magnetomicelle-bound enzymes could be recycled and reused without contamination from prior reactions, we designed a transcription assay using T7 RNAP–magnetomicelles and the two different DNA templates (for 135-nt mRNA and 76-nt tRNA<sup>Pro</sup>) described above. The first reaction was performed in the presence of one DNA template, followed by magnetic separation of the T7 RNAP–magnetomicelles, removal of the RNA product generated, washing, and a second transcription with the separated bioconjugates and the opposite DNA template (Figure 5a). Incomplete washing of the recycled T7 RNAP–magnetomicelles would be assayed by the production of the first RNA product in the second reaction. As a result, up to four T7 RNAP–magnetomicelle washes were required to remove DNA contamination in a second reaction (34). To our surprise, T7 RNAP–magnetomicelles successfully transcribed RNA up to three times, although only the first two reactions produced levels of RNA with no qualitative loss in T7 RNAP activity (Figure 5b). Additionally, the amount of RNA produced from recycled T7 RNAP was dependent on the concentration of T7 RNAP conjugated to the magnetomicelle surface. The recovery and reuse of T7 RNAP is significant, considering the complexity of the transcription reaction and the fragility of T7 RNAP.

## DISCUSSION

Nanoparticle-supported proteins have considerable potential in a variety of biotechnological areas, mostly limited by the bioconjugation chemistries available for joining proteins and particles and the biocompatibility of the protein for the solid support. In the present study, we have proposed a new composite nanostructure suitable for protein bioseparation and enzymatic recycling. Our method takes advantage of IMAC chemistry and requires His<sub>6</sub>-tagged recombinant proteins for attachment to encapsulated, magnetic  $\gamma$ -Fe<sub>2</sub>O<sub>3</sub> particles. Specifically, using His<sub>6</sub>-tagged T4 DNAL, we demonstrated reproducible binding capacity on the surface of the magnetomicelles and specific protein capture through the His<sub>6</sub>-Cu<sup>2+</sup>-IDA interaction. This highly specific protein attachment is likely a factor for the retention of enzyme function in subsequent experiments. We argue that these nanoparticle supports should be versatile, as the carboxylic acid groups available on the surface of the magnetomicelles could be further functionalized to recognize other distinctive protein features for bioconjugation and could in turn provide additional scenarios for specific protein capture.

Additionally, by quantifying the amount of His<sub>6</sub>-EGFP conjugated to a magnetomicelle surface, we revealed large loading capacities of bound, intact protein. The high surface-to-volume ratio afforded by conjugating proteins to nanoparticle supports is a clear advantage over other solid-supported enzyme techniques. Furthermore, the Cu<sup>2+</sup>-IDA magnetomicelles utilized in these examples were prepared by cross-linking 50% of available carboxylic acid groups prior to Cu<sup>2+</sup>-IDA functionalization and subsequent protein attachment. We envision that this system could be modified to accommodate more or fewer IDA groups to tailor the number of conjugated proteins.

Most importantly, Cu<sup>2+</sup>-IDA magnetomicelles were bio-compatible in transcription reactions performed with bound T7 RNAP, with only subtle losses in enzyme activity. This lower activity could be due to enzyme denaturation or a structural change at the particle surface, as has been previously demonstrated for adsorbed protein–nanoparticle conjugates (10), or a portion of the bound protein may be less accessible for catalysis than in free solution. Although the loss in RNA production after T7 RNAP bioconjugation to magnetomicelles was not favorable, we are optimistic that magnetomicelle supports could be applicable for the conjugation of other proteins. Reports of catalyst activity on magnetic supports is diverse for particle-bound enzymes, ranging from a significant or complete loss in activity to an increase in catalytic function (41, 46–48). Therefore, despite the variability in surface-bound enzyme activity, there remains great interest in the potential for magnetic enzyme carriers that permit easy enzyme separation and reuse.

Recyclable biocatalysts are becoming more widely used for organic transformations in industrially relevant reactions (6). Our work, by contrast, is one of the first examples of magnetic recycling of an enzyme used in a molecular biology transformation under strict biological conditions. In principle, our enzyme–magnetomicelle system could be broadly applied for the separation and reuse of a variety of enzymes under diverse reaction conditions. In addition to the advantages that protein–magnetomicelles offer to protein separation, analysis, and enzyme reuse, we envision that proteins attached to the surface of magnetomicelles could also facilitate targeted, magnetic drug delivery (49) or be used in *in vivo* imaging systems (50, 51).

## ACKNOWLEDGMENT

We would like to acknowledge the NIH (EB003809) for support of this research; A.R.H. also acknowledges Abbey E. Rosen and the Karin Musier-Forsyth group for their generous gift of the tRNA<sup>Pro</sup> plasmid DNA, as well as clones for T4

DNAL and T7 RNAP. Additionally, A.R.H. would also like to thank Jennifer Maynard for the EGFP clone. K.B.S. thanks Dr. Taewoon Cha for XPS analysis.

**Supporting Information Available:** Additional figures. This material is available free of charge via the Internet at <http://pubs.acs.org>.

## LITERATURE CITED

- Niemeyer, C. M. (2001) Nanoparticle, proteins, and nucleic acids: biotechnology meets materials science. *Angew. Chem., Int. Ed.* **40**, 4128–4158.
- Gao, X., Cui, Y., Levenson, R. M., Chung, L. W., and Nie, S. (2004) In vivo cancer targeting and imaging with semiconductor quantum dots. *Nat. Biotechnol.* **22**, 969–76.
- Xiao, Y., Patolsky, F., Katz, E., Hainfeld, J. F., and Willner, I. (2003) “Plugging into enzymes”: nanowiring of redox enzymes by a gold nanoparticle. *Science* **299**, 1877–1881.
- Tannous, B. A., Grimm, J., Perry, K. F., Chen, J. W., Weissleder, R., and Breakefield, X. O. (2006) Metabolic biotinylation of cell surface receptors for in vivo imaging. *Nat. Methods* **3**, 391–396.
- Cao, L., van Langen, L., and Sheldon, R. A. (2003) Immobilized enzymes: carrier-bound or carrier-free? *Curr. Opin. Biotechnol.* **14**, 387–394.
- Bornscheuer, U. T. (2003) Immobilizing enzymes: How to create more suitable biocatalysts. *Angew. Chem., Int. Ed.* **42**, 3336–3337.
- You, C.-C., Verma, A., and Rotello, V. M. (2006) Engineering the nanoparticle-biomacromolecule interface. *Soft Matter* **2**, 190–204.
- Carpenter, E. E. (2001) Iron nanoparticles as potential magnetic carriers. *J. Magn. Magn. Mater.* **225**, 17–20.
- Li, J., Wang, J., Gavalas, V. G., Atwood, D. A., and Bachas, L. G. (2003) Alumina-pepsin hybrid nanoparticles with orientation-specific enzyme coupling. *Nano Lett.* **3**, 55–58.
- Vertegel, A. A., Siegel, R. W., and Dordick, J. S. (2004) Silica nanoparticle size influences the structure and enzymatic activity of adsorbed lysozyme. *Langmuir* **20**, 6800–6807.
- Lei, C., Shin, Y., Liu, J., and Ackerman, E. J. (2002) Entrapping enzyme in a functionalized nanoporous support. *J. Am. Chem. Soc.* **124**, 11242–11243.
- Kulkarni, S., Schilli, C., Mueller, A. H. E., Hoffman, A. S., and Stayton, P. S. (2004) Reversible meso-scale smart polymer–protein particles of controlled sizes. *Bioconjugate Chem.* **15**, 747–753.
- Huang, S.-H., Liao, M.-H., and Chen, D.-H. (2003) Direct binding and characterization of lipase onto magnetic nanoparticles. *Biotechnol. Prog.* **19**, 1095–1100.
- Johnson, D. L., and Martin, L. L. (2005) Controlling protein orientation at interfaces using histidine tags: an alternative to Ni/NTA. *J. Am. Chem. Soc.* **127**, 2018–2019.
- Lata, S., and Piehler, J. (2005) Stable and functional immobilization of histidine-tagged proteins via multivalent chelator headgroups on a molecular poly(ethylene glycol) brush. *Anal. Chem.* **77**, 1096–1105.
- Wang, Y., and Caruso, F. (2005) Mesoporous silica spheres as supports for enzyme immobilization and encapsulation. *Chem. Mater.* **17**, 953–961.
- Meziani, M. J., Pathak, P., Harruff, B. A., Hurezeanu, R., and Sun, Y.-P. (2005) Direct conjugation of semiconductor nanoparticles with proteins. *Langmuir* **21**, 2008–2011.
- Xu, C., Xu, K., Gu, H., Zhong, X., Guo, Z., Zheng, R., Zhang, X., and Xu, B. (2004) Nitrotriacetic acid-modified magnetic nanoparticles as a general agent to bind histidine-tagged proteins. *J. Am. Chem. Soc.* **126**, 3392–3393.
- Xu, C., Xu, K., Gu, H., Zheng, R., Liu, H., Zhang, X., Guo, Z., and Xu, B. (2004) Dopamine as a robust anchor to immobilize functional molecules on the iron oxide shell of magnetic nanoparticles. *J. Am. Chem. Soc.* **126**, 9938–9939.
- Kim, B.-S., Qiu, J.-M., Wang, J.-P., and Taton, T. A. (2005) Magnetomicelles: composite nanostructures from magnetic nanoparticles and cross-linked amphiphilic block copolymers. *Nano Lett.* **5**, 1987–1991.
- Abad, J. M., Mertens, S. F. L., Pita, M., Fernandez, V. M., and Schiffrin, D. J. (2005) Functionalization of thioctic acid-capped gold nanoparticles for specific immobilization of histidine-tagged proteins. *J. Am. Chem. Soc.* **127**, 5689–5694.
- Ausubel, F. M. B. R., Kingston, R. E., Moore, D. D., Seidman, J. G., Smith, J. A., Struhl, K. (1999) *Short Protocols in Molecular Biology*, 4th ed., John Wiley & Sons: New York.
- Strobel, S. A., and Cech, T. R. (1995) Minor groove recognition of the conserved G.U pair at the *Tetrahymena* ribozyme reaction site. *Science* **267**, 675–9.
- Cormack, B. P., Valdivia, R. H., and Falkow, S. (1996) FACS-optimized mutants of the green fluorescent protein (GFP). *Gene* **173**, 33–38.
- Ellinger, T., and Ehrlich, R. (1998) Single-step purification of T7 RNA polymerase with a 6-histidine tag. [Erratum to document cited in CA129:64701]. *BioTechniques* **25**, 640.
- Stehlin, C., Burke, B., Yang, F., Liu, H., Shiba, K., and Musier-Forsyth, K. (1998) Species-specific differences in the operational RNA code for aminoacylation of tRNA<sup>Pro</sup>. *Biochemistry* **37**, 8605–8613.
- Kang, Y., and Taton, T. A. (2005) Controlling shell thickness in core-shell gold nanoparticles via surface-templated adsorption of block copolymer surfactants. *Macromolecules* **38**, 6115–6121.
- Kang, Y., and Taton, T. A. (2005) Core/shell gold nanoparticles by self-assembly and crosslinking of micellar, block-copolymer shells. *Angew. Chem., Int. Ed.* **44**, 409–412.
- Porath, J., Carlsson, J., Olsson, I., and Belfrage, G. (1975) Metal chelate affinity chromatography, a new approach to protein fractionation. *Nature (London)* **258**, 598–9.
- Chaga, G. S. (2001) Twenty-five years of immobilized metal ion affinity chromatography: past, present and future. *J. Biochem. Biophys. Methods* **49**, 313–334.
- Lee, K. B., Park, S., and Mirkin, C. A. (2004) Multicomponent magnetic nanorods for biomolecular separations. *Angew. Chem., Int. Ed.* **43**, 3048–3050.
- Pack, D. W., Chen, G. H., Maloney, K. M., Chen, C. T., and Arnold, F. H. (1997) A metal-chelating lipid for 2D protein crystallization via coordination of surface histidines. *J. Am. Chem. Soc.* **119**, 2479–2487.
- Shnek, D. R., Pack, D. W., Sasaki, D. Y., and Arnold, F. H. (1994) Specific protein attachment to artificial membranes via coordination to lipid-bound copper(II). *Langmuir* **10**, 2382–2388.
- See Supporting Information for details.
- Dai, J., Bao, Z., Sun, L., Hong, S. U., Baker, G. L., and Bruening, M. L. (2006) High-capacity binding of proteins by poly(acrylic acid) brushes and their derivatives. *Langmuir* **22**, 4274–4281.
- Schmid, E. L., Keller, T. A., Dienes, Z., and Vogel, H. (1997) Reversible oriented surface immobilization of functional proteins on oxide surfaces. *Anal. Chem.* **69**, 1979–1985.
- Cha, T., Guo, A., Jun, Y., Pei, D., and Zhu, X.-Y. (2004) Immobilization of oriented protein molecules on poly(ethylene glycol)-coated Si(111). *Proteomics* **4**, 1965–1976.
- Tanaka, M., and Sackmann, E. (2005) Polymer-supported membranes as models of the cell surface. *Nature (London)* **437**, 656–663.
- Anikin, K., Roecker, C., Witemann, A., Wiedenmann, J., Ballauff, M., and Nienhaus, G. U. (2005) Polyelectrolyte-mediated protein adsorption: fluorescent protein binding to individual polyelectrolyte nanospheres. *J. Phys. Chem. B* **109**, 5418–5420.
- Yang, F., Moss, L. G., and Phillips, G. N. (1996) The molecular structure of green fluorescent protein. *Nat. Biotechnol.* **14**, 1246–1251.
- Dyal, A., Loos, K., Noto, M., Chang, S. W., Spagnoli, C., Shafi, K. V. P. M., Ulman, A., Cowman, M., and Gross, R. A. (2003) Activity of *Candida rugosa* lipase immobilized on  $\gamma$ -Fe<sub>2</sub>O<sub>3</sub> magnetic nanoparticles. *J. Am. Chem. Soc.* **125**, 1684–1685.
- Long, M. S., and Keating, C. D. (2006) Nanoparticle conjugation increases protein partitioning in aqueous two-phase systems. *Anal. Chem.* **78**, 379–386.
- Jia, H., Zhu, G., and Wang, P. (2003) Catalytic behaviors of enzymes attached to nanoparticles: the effect of particle mobility. *Biotechnol. Bioeng.* **84**, 406–414.
- Phadtare, S., Vinod, V. P., Mukhopadhyay, K., Kumar, A., Rao, M., Chaudhari, R. V., and Sastry, M. (2004) Immobilization and

- biocatalytic activity of fungal protease on gold nanoparticle-loaded zeolite microspheres. *Biotechnol. Bioeng.* 85, 629–637.
- (45) Chamberlin, M., and Ring, J. (1973) Characterization of T7-specific ribonucleic acid polymerase. II. Inhibitors of the enzyme and their application to the study of the enzymatic reaction. *J. Biol. Chem.* 248, 2245–50.
- (46) Rossi, L. M., Quach, A. D., and Rosenzweig, Z. (2004) Glucose oxidase-magnetite nanoparticle bioconjugate for glucose sensing. *Anal. Bioanal. Chem.* 380, 606–613.
- (47) Krogh, T. N., Berg, T., and Hojrup, P. (1999) Protein analysis using enzymes immobilized to paramagnetic beads. *Anal. Biochem.* 274, 153–162.
- (48) Kouassi, G. K., Irudayaraj, J., and McCarty, G. (2005) Examination of cholesterol oxidase attachment to magnetic nanoparticles. *J. Nanobiotechnol.*, 3:1.
- (49) Son, S. J., Reichel, J., He, B., Schuchman, M., and Lee, S. B. (2005) Magnetic nanotubes for magnetic-field-assisted bioseparation, biointeraction, and drug delivery. *J. Am. Chem. Soc.* 127, 7316–7317.
- (50) Lewin, M., Carlesso, N., Tung, C.-H., Tang, X.-W., Cory, D., Scadden, D. T., and Weissleder, R. (2000) Tat peptide-derivatized magnetic nanoparticles allow in vivo tracking and recovery of progenitor cells. *Nat. Biotechnol.* 18, 410–414.
- (51) Xie, H.-Y., Zuo, C., Liu, Y., Zhang, Z.-L., Pang, D.-W., Li, X.-L., Gong, J.-P., Dickinson, C., and Zhou, W. (2005) Cell-targeting multifunctional nanospheres with both fluorescence and magnetism. *Small* 1, 506–509.

BC060215J